JOURNAL OF NEUROPHYSIOLOGY
Vol. 70, No. 1, July 1993. *Printed in U.S.A.*

Motor Cortical Activity During Drawing Movements: Population Representation During Sinusoid Tracing

ANDREW B. SCHWARTZ
Division of Neurobiology, Barrow Neurological Institute, Phoenix, Arizona 85013

SUMMARY

1. Monkeys were trained to trace sinusoids with their index fingers on a planar surface. During this task, both the direction and speed of movement varied continuously. Activity of individual units in the precentral gyrus contralateral to the moving arm was recorded as the task was performed. These cells responded to passive movement of the shoulder and/or elbow. The relation between discharge rate and movement direction for these individual cells could be described with a cosine tuning function.

2. Data recorded as the sinusoid was traced were divided into 100 bins as each cell was studied during the experiment. In each bin, the activity of a particular cell was represented by a vector. The vector ("cell vector") pointed in the direction of finger movement that corresponded to the highest rate of neuronal discharge. This direction, referred to as the preferred direction, corresponded to the peak of the cosine tuning function. The direction of the vector was constant between bins, but the magnitude of this cell's vector was a function of the instantaneous discharge rate.

3. This cell vector is a hypothetical contribution of a single cell to the population response comprised of 554 similarly derived vectors from different cells. The population response was represented as the vector that resulted from forming the sum of the vector contributions from the individual cells. A separate calculation was made for each bin, resulting in 100 population vectors for each sinusoid.

4. Within a given time series of population vectors, their lengths and directions varied in a consistent relation to the tangential velocity of the drawing movement. Therefore these vectors are representative of the movement trajectory. Each increment of a trajectory was predicted by a population vector that preceded it by ~120 ms. These findings suggest that trajectory information is encoded in an ongoing manner in the motor cortex using a relative coordinate system that moves in conjunction with the finger.

INTRODUCTION

Previous investigations examining volitional arm movements have shown that the activity of most task-related neurons in the precentral cortex is strongly influenced by the direction of movement. This can be represented by a cosine tuning function that spans all directions of movement. Thus, for any given change of movement direction, the frequency of discharge in many cells will change simultaneously. A population vector model has been used to represent the emergent directional information from this group of cells. Population vectors predict accurately the direction of reaching movements in two- and three-dimensional space (Georgopoulos et al. 1983, 1988).

The purpose of the present experiment was to examine the temporal characteristics of motor cortical activity within an arm movement. The trajectory of movement is the time pattern of limb displacement. Because trajectory is explicitly specified in drawing movements, this class of movement is ideally suited for testing the hypothesis of this study: is trajectory represented in the temporal pattern of unitary activity in motor cortex? Sinusoid drawing was chosen because both the speed and direction of movement change continuously as the figure is drawn. Because the method in this study utilizes vectors to represent the trajectory, both the direction and the magnitude (equivalent to speed in this case) of the vector must be encoded in the cortical activity for an affirmative answer to the hypothesis. In a previous paper that detailed the characteristics of single-cell activity during this task, it was shown that much of the activity pattern could be accounted for by movement direction (Schwartz 1992). Speed of movement accounted for a smaller portion of the discharge pattern. Neither the tuning function relating direction to discharge nor the speed-discharge relation was precise enough to accurately predict the movement trajectory. The speed-discharge pattern was most robust when the direction of movement was near the cell's preferred direction. In contrast, the population vector techniques used in the present paper show that an accurate representation of both direction and speed emerge from the population. Speed is directly proportional to the magnitude of the population vector. Because both parameters are simultaneously represented in the population vector, this vector is a predictor of the tangential velocity generated in this task. The shape of the drawn figure can be extracted from the calculated time series of population vectors.

METHODS

The general methods used in this study, including those for the surgical, recording, and data acquisition procedures as well as the behavioral paradigm, were detailed in a previous report (Schwartz 1992).

Behavior and recording paradigm

Rhesus monkeys were trained to trace with their index fingers on a touch-sensitive computer monitor. The monkeys became proficient at two tasks. The center→out task was a set of conditions that required the animal to begin a movement in the center of the screen and move directly to one of eight targets arranged at equal spatial intervals around a circle with a 6-cm radius. Direct movements to each of the eight peripheral targets were repeated in a random order five times per experimental run. The monkeys performed the other task (tracing task) by tracing horizontally oriented sinusoids across the screen. The sinusoids consisted of five different combinations of amplitude and spatial frequency. Each combination was traced both leftward and rightward across the screen for a total of 10 different experimental classes. The trial began with the appearance of a target circle at one margin of the

screen. When the animal held its finger in this target, one of five sinusoids would then be presented, originating at the target circle. The target would jump along the figure and the animal would then be required to move its finger along the screen to this location within ~150 ms. The animals learned to perform smooth, graceful movements that were within 1 cm of the projected figure. Movement speed was determined by the animal, because the target circle jumped to the next location along the figure as soon as it was acquired by the animal. After training, a chronic recording chamber was implanted in the skull over the proximal arm area of the motor cortex contralateral to the arm used for the task. Single units that responded when the shoulder and/or elbow was passively manipulated, that were active in the task, and that could be fit with a cosine tuning function during the center→out task were included in the analysis.

Analysis

Spike data generated from five repetitions of movements to each target recorded during the center→out task were regressed to a cosine formula, as described previously (Schwartz 1992). This formula characterized the pattern of discharge across all directions of movement. Tuned cells, by definition, had the highest discharge rate when the finger moved in the cell's preferred direction, and had progressively lower rates for movements in directions more remote from this direction of peak firing. A set of rasters from a single cell illustrates this relation in Fig. 1*A*. These rasters arranged around a center start position and located in the direction of movement show that this cell tended to have high discharge rates when the movement direction was down and to the left. The preferred direction determined from the regression analysis was 254° (*down* and *leftward*) in the coordinate system used in this analysis. Histograms of cell activity during the sinusoid tracing were calculated by dividing each trial into 100 bins. The experimental epoch over which this was calculated started 120 ms before the finger moved from the initial hold position and ended 120 ms before the task was completed. Fractional interspike intervals were calculated for each bin and averaged across repetitions. The fractional intervals were converted to discharge rates by dividing each bin by the average bin duration (average trial time/100). Population vectors, P_t, were calculated for each bin by taking a unit vector, C_i, pointing in the preferred direction of each cell, i, and setting its magnitude with the weighting function

$$w_{i,t} = \frac{D_{i,t} - \bar{D}_i}{D_{max_i} - D_i}$$

where $D_{i,t}$ is the discharge rate in bin t of cell i, $\bar{D}_i$ is the geometric mean for cell i and D_{max_i} is the maximum discharge rate for the cell. The population vector was calculated by taking the vector average of the N-weighted cell vectors

$$\vec{P}_t = \frac{\sum_{i=1}^{N} w_{i,t}\vec{C}_i}{N}$$

A histogram of firing rates during the tracing task from the cell represented in Fig. 1*A* is shown as an example in Fig. 1*B*. The unit vector is weighted by $w_{i,t}$, and the time series of weighted vectors is shown on the *right*. The small arrow shows where the movement began (~120 ms from the beginning of the spike data). The population vector for the first spike data bin was constructed by summing weighted vectors from 544 different cells, shown on the *right* of Fig. 1*C*. The small arrowhead marks the contribution of the cell shown in Fig. 1, *A* and *B*, whereas the heavy line represents P_t, the population vector for the first bin. Notice that this population vector, constructed 120 ms before the movement began, points in the same direction as the initial movement direction shown on the *left* of Fig. 1*C*.

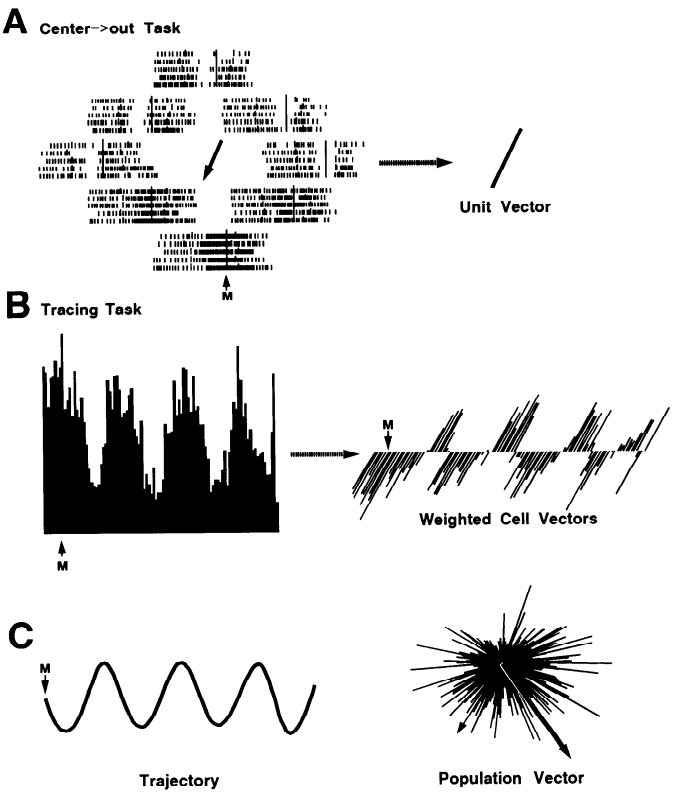

FIG. 1. Population method. *A*: rasters derived from the center→out task were used to calculate a cell's preferred direction. Each raster represents 5 repetitions of a movement from the center of the figure to a target located at the raster's position. The rasters are aligned to movement onset. The average discharge rate during the reaction and movement time was greatest for movements down and to the left. The Euclidean coordinate system used throughout this paper is oriented with 0° along the positive x axis and 90° upward. The preferred direction of this unit was 254°, and is represented by the arrow in the *middle* of the figure. This procedure yields a unit vector pointing in the cell's preferred direction. *B*: instantaneous discharge rate during the sinusoid tracing was calculated in 100 bins as represented in the histogram. Spike data were aligned to a sync point 120 ms before the finger exited the start location on the touchscreen. The unit vector weighted by the discharge rate was used to calculate a cell vector for each bin. *C*: same procedure was carried out for all 554 cells in the population. The result for the 1st bin of class 1 is represented as a cluster of cell vectors. The population vector (not to scale) resulting from the vector addition of the 554 clusters is represented as the heavy arrow. Small arrow: vector contribution of the unit displayed in *A* and *B*. The direction of the population vector matches the initial direction of the trajectory.

The time series of population vectors could be added tip-to-tail to create a neural representation of the trajectory. To compare this representation with the actual trajectory, the x and y components of the neural trajectory were normalized to the finger trajectory. This was carried out for each class using the maximum and minimum x and y components of each time series to define the normalization factors

$$x_{norm} = \frac{xpop_{max} - xpop_{min}}{xdisp_{max} - xdisp_{min}}$$

$$y_{norm} = \frac{ypop_{max} - ypop_{min}}{ydisp_{max} - ydisp_{min}}$$

These x and y components of each population vector were then divided by the respective constants to convert their units from spikes per bin to centimeters per bin.

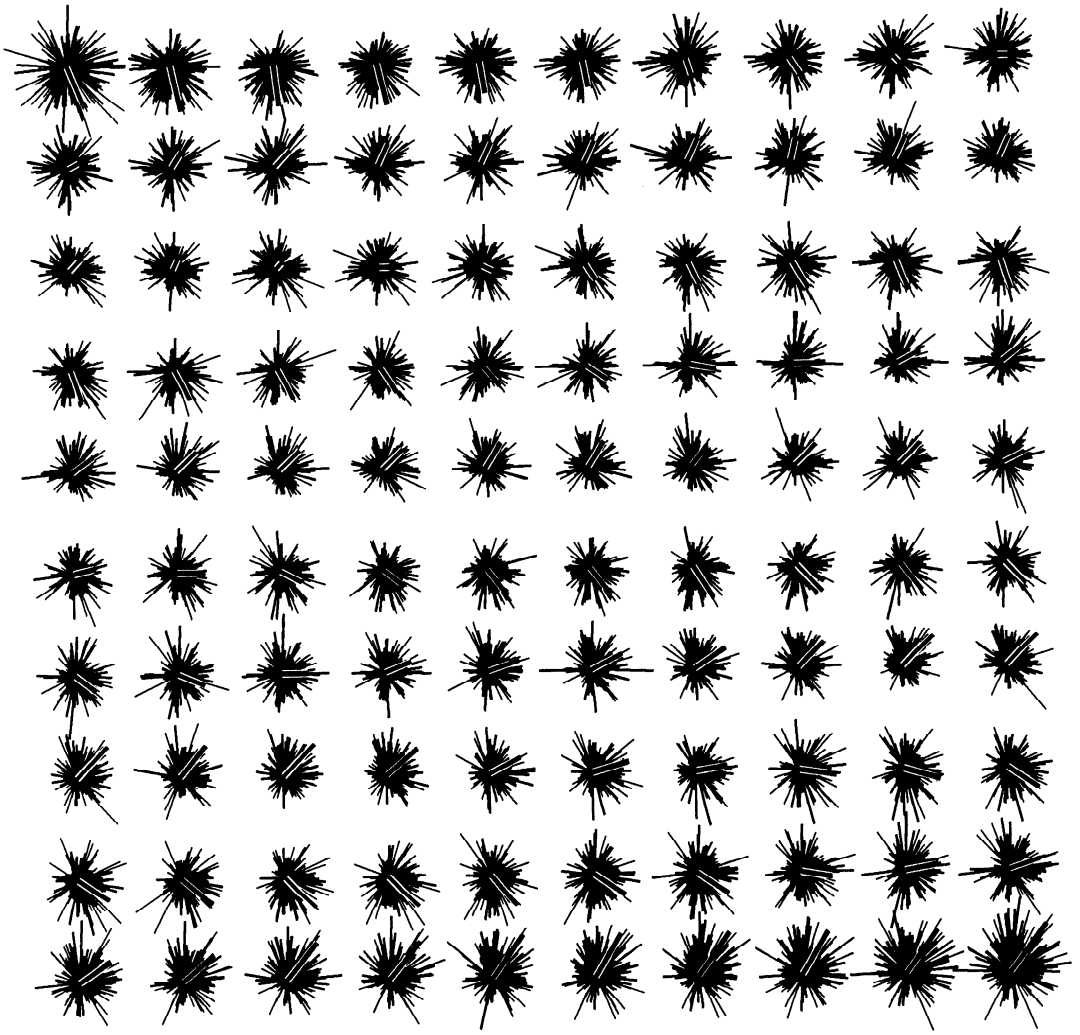

FIG. 2. Population clusters. Clusters consisting of 554 cell vectors are displayed in serial order (*left* to *right* and *top* to *bottom*) for the class 1 sinusoid. Heavy lines: population vectors. Small symmetrical clusters yield short population vectors, and these tend to occur for horizontal directions corresponding to slow speeds.

RESULTS

A series of 100 population clusters for the class 1 sinusoid (amplitude = 3 cm, 3 cycles per screen, drawn rightward) is shown in Fig. 2. The clusters are presented in temporal order from *left* to *right* and *top* to *bottom*. The thin lines represent the cell vectors from each of the 554 neurons that contribute to the population vector. The first cluster was calculated 120 ms before the finger moved from the start location. In general, the length of the population vector is related to the asymmetry of the cluster. The directions and magnitudes of the population vectors change gradually. The shortest vectors are always pointing horizontally and have symmetrical, compact clusters. The finger was moving horizontally only at the peaks of the sinusoids, and this was the region of the figure where the curvature was highest. Because curvature and speed are inversely related, the short population vectors that emerge from the symmetrical clusters are consistent with low movement speeds. The temporal variation in population vector direction and magnitude is illustrated in Fig. 3 for the 10 classes of sinusoids. This pattern can be compared directly to the series of tangential velocity vectors in Fig. 4. It is apparent that both the directions and magnitudes of the population vectors are quite similar to those of the corresponding velocity vectors. In classes 1–3 and 6–8, the radius of curvature at the peak of the sinusoids was small and the tangential speed was also small. The metrics of the population and velocity vectors corresponded between classes as well as within the temporal sequence of a given class.

The relation between the population vector direction and the direction of the velocity vectors was examined quantitively by cross correlation. Usually, standard correlation techniques cannot be applied to directional data because the coordinate system is circular, i.e., 359° is only 2° from 1°. However, the coordinate system used in this experiment, with 0° along the positive x axis and 90° along the positive y axis, along with the fact that only two quadrants were traversed as each horizontal sinusoid was traced, made this standard comparison possible. For the sinusoids traced from *left* to *right* (classes 6–10), the fourth and first quadrants were traversed, and, to make the coordinates continuous, the fourth quadrant was remapped from 270 through 360° to −90 through 0°. Thus classes 6–10 have movement directions that range from −90 to +90°. Classes 1–5 traversed the second and third quadrants (90–270°) and were not remapped. The movement and population vector direc-

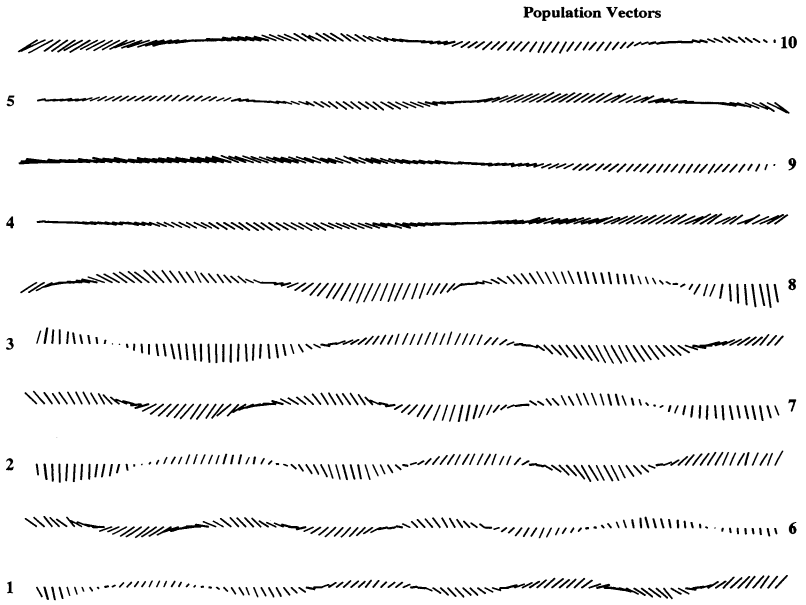

FIG. 3. Population vectors. The population response for each sinusoid class is represented in each sequence of 100 vectors. The class number beside each sequence is located at the origin. Classes 1–5 were drawn from *left* to *right*, and classes 6–10 in the opposite direction. The 1st vector of each sequence was derived from spike data that started 120 ms before the finger exited the start location.

tions are compared for each sinusoid class in Fig. 5*A*. In this figure, the population vector direction is shifted by 120 ms to align better to the direction of movement. The correspondence between the two traces is very good, with minor differences for classes 1–3 and 6–8 near the beginning of the task. The correllograms for this directional comparison are shown in Fig. 5*C*. The peak correlations have values from 0.91 to 0.96 and occur with a lag of 102–136 ms. Using the lag for each class, the traces shown in Fig. 5*A* were shifted and subtracted. The resulting differences are displayed in Fig. 5*B* (note the scale difference between 5, *A* and *B*). The largest differences occurred near the beginning of the movement for classes 1–3 and 6–8.

The same analysis was carried out for speed (length of the velocity vector) and the magnitude of the population vector. The maximum population vector length for each class was normalized to the largest speed for the corresponding sinusoid. These traces, with the population vector lengths shifted by 120 ms, are shown in Fig. 6*A*. Again, the correspondence within the pairs of traces is very good. There is little variation in speed for classes 4 and 9 because these sinusoids were of low amplitude with a large radius of curvature near the peak. The correllograms displayed in Fig. 6*C* have peak values that range from 0.50 to 0.86 and have lags of 102–151 ms. After the traces were shifted by their lags and subtracted, the resulting differences were evenly distributed throughout each trial (Fig. 6*B*).

Because both direction and speed were well represented in the series of population vectors, it was possible to construct "neural trajectories" by adding the population vectors for each class tip-to-tail. The result is plotted on the *right* of Fig. 7, with the actual trajectories plotted on the *left*. Except for the initial portions of classes 1–3 and 6–8, the neural trajectories are quite similar to those of the finger. In the classes with the aberrant initial portions, the distortion is largest at the first peak of each sinusoid. This corresponds to the largest difference angle for these classes displayed in Fig. 5*B*.

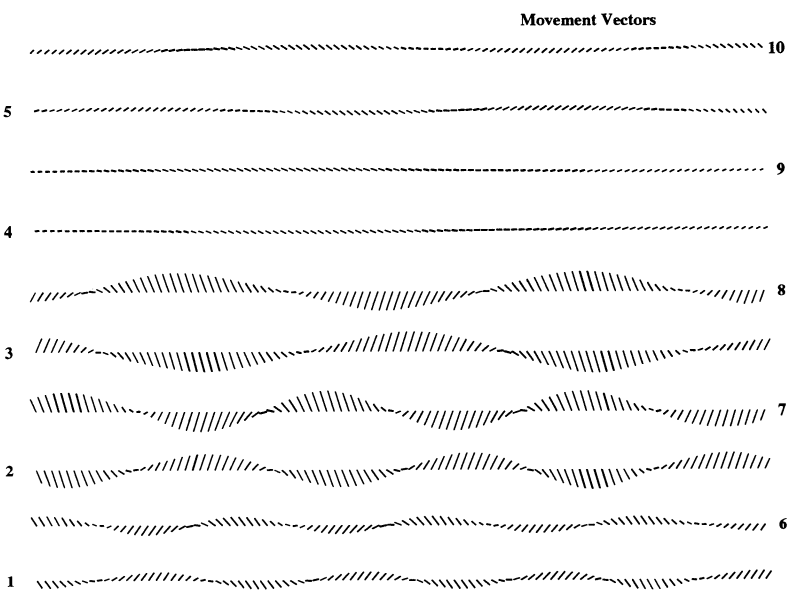

FIG. 4. Movement vectors. The tangential velocity vectors are presented in the same format as the population vectors of Fig. 3. These vectors derived from finger movement correspond closely to the population vectors. The 1st vector was calculated from the finger positions on exit from the start location.

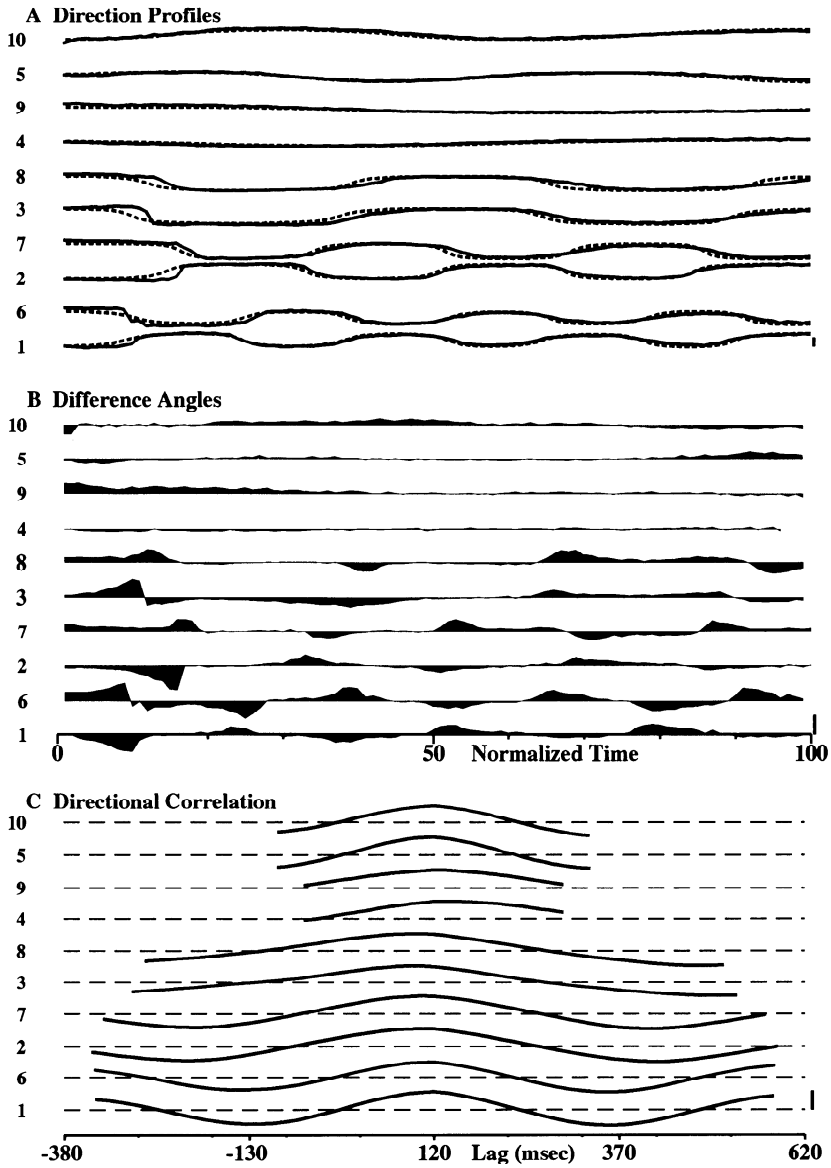

FIG. 5. Population vector direction vs. movement direction. *A*: population vector direction is plotted as the heavy line and movement direction as the light line. The abscissa is normalized movement time (100 bins). The numbers to the *left* of each trace are the class numbers. These traces are derived from the data illustrated in Figs. 3 and 4. The vertical calibration bar represents 90°. For classes 1–5, the y values of the figure range from 90 to 270°. The values of classes 6–10 range from −90 to +90°. Population vector direction corresponds closely to movement direction. *B*: traces in *A* were shifted by their cross-correlation lags (Fig. 5*C*) and subtracted. The differences (population − movement) are largest at the beginning of the task. The scale is magnified relative to *A* (calibration bar = 90°). *C*: cross-correlograms of movement direction relative to population vector direction show that the 2 were well correlated and that the lag for each class was near 120 ms. The time scale along the abscissa was calculated from the normalized data by equating the average duration for each class to bin 100. The calibration bar is $r = 1.0$.

The variability in the performance of the task was calculated with a bootstrapping technique (Diaconis and Efron 1983; Georgopoulos et al. 1988). Selections from the database of 554 experiments were made randomly 554 times; a particular selection could be made more than once. Each selection consisted of 100 bins of normalized x-y touchscreen data acquired as the sinusoid was traced. The selected data were used to calculate an average trajectory for each sinusoid class. This process was repeated 100 times, and the resulting 100 trajectories were rank ordered by their root-mean-squared difference from the overall mean trajectory. The trajectory that was ranked as 95 represented the confidence interval containing 95% of the variability. Each velocity vector of this trajectory was broken into x and y components and displayed in Fig. 8. An ellipse was plotted for each bin of the mean trajectory. The axis of the ellipse in the x dimension represents the variability in the x direction, and the y axis represents y variability. The variability was so small relative to the metrics of the trajectory that each ellipse was magnified by a factor of 20. The variability of the trajectory was greatest in the portions of the sinusoid with greatest curvature.

The same technique was used to measure the variability of the neural trajectories. Selections were made 554 times, and a time series of 100 population vectors was calculated for each sinusoid class. This process was repeated 100 times, resulting in 100 neural trajectories that were rank ordered in the same way as the finger trajectories. The resulting variability in the x and y dimensions was represented by ellipses located at the end of each preceding mean population vector. The ellipses representing the 95% confidence interval in Fig. 9 were magnified 5 times relative to the mean neural trajectory. The variability tended to change by region through the trajectory—large ellipses were in the same part of the trajectory. There was also a tendency for the largest variability to occur at the beginning of each movement. Within the neural trajectories, the pattern of variability differed from the pattern observed in the finger trajectories.

DISCUSSION

In general, volitional movement is associated with a set of parameters that change continuously throughout the

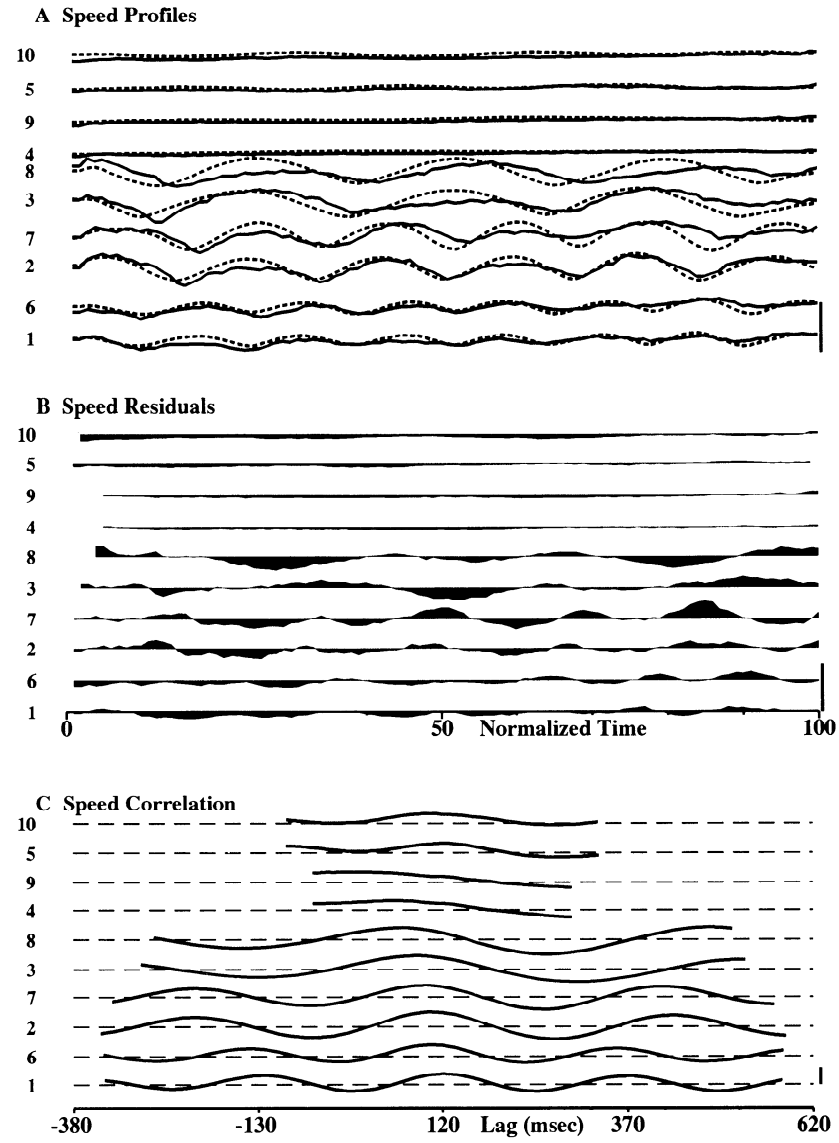

FIG. 6. Population vector length vs. movement speed. *A*: normalization factor was found when the maximum population vector magnitude [SQRT($x^2 + y^2$)] for each class was divided by the maximum speed encountered in that class. The population vector length (——) was multiplied by this factor and shifted by 120 ms before being matched to the finger speed (- - -). The calibration bar is 50 cm/s. *B*: population trace was shifted by its correlation lag (Fig. 6*C*) and the speed trace subtracted. The differences were evenly distributed through the task. The scale is the same as in *A*. *C*: correlograms showing the correlation between the 2 traces were centered near a lag of 120 ms. The vertical bar is $r = 1.0$.

movement. Drawing is characterized by its path or trajectory, and the production of this path in time can be completely described with the parameters of direction and speed. The purpose of this study was to determine whether, and how well, these parameters were encoded in the activity of motor cortical neurons.

Previous research has shown that the average activity of individual neurons of the motor cortex varies with the constant direction of straight arm movements (Georgopoulos et al. 1982), with a cosine tuning function between movement direction and discharge rate. A recent study (Schwartz 1992) showed that this relation was valid for drawing movements when direction and discharge activity were considered instantaneously. To test the hypothesis that movement is accurately represented in the motor cortex as a figure is drawn, it would be desirable to use the cortical activity to predict the actual movement. The tuning function for individual neurons, however, cannot by itself be used to predict movement direction because two directions are coded for each discharge rate (except at the peak) and the function is broad, spanning the entire directional domain. In contrast, the population vector algorithm utilizes the preferred direction derived from the tuning curves of many individual cells and does yield an accurate prediction of movement direction. Previously, population vectors derived from neuronal activity were shown to predict well the direction of straight reaching movements (Georgopoulos et al. 1983; Schwartz et al. 1988). Population vectors generated continuously during a pointing task in three-dimensional space were shown to represent well the trajectories of these relatively straight movements (Georgopoulos et al. 1988). A movement trajectory can be described by a series of tangent vectors, each of which points in an instantaneous direction and has a magnitude proportional to the speed of the movement. These vectors were found by dividing the movement trajectory into segments at equal temporal intervals. The resulting series of vectors was then compared with the corresponding series of population vectors, which were shown to predict well both direction and speed as they changed continuously through the movement.

In this algorithm, each cell makes a contribution to the population in the cell's preferred direction. This contribution is weighted by a factor proportional to the discharge

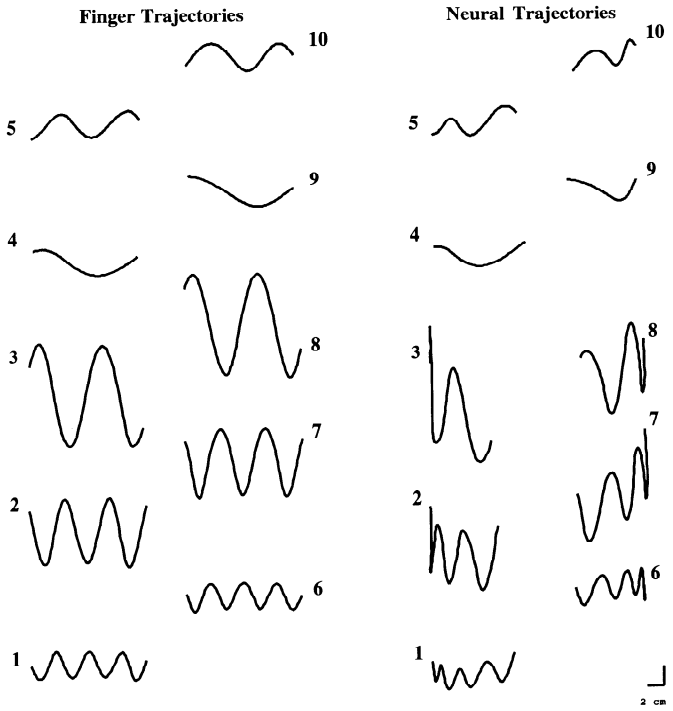

FIG. 7. Trajectories. The population vectors of Fig. 3 and the velocity vectors of Fig. 4 were added tip-to-tail to form neural (*right*) and finger trajectories (*left*). The procedure for normalizing the population vectors is described in the text. Class labels are positioned at the origin of each trace. The calibration bars are 2 cm.

rate at the instant the population vector is calculated. Directional information encoded by individual cells is summed, resulting in a population vector oriented in the direction of movement that will occur ~120 ms later. Speed, as compared with direction, is more poorly encoded in single cells, yet the neuronal population as a whole accurately encodes speed information. The speed at a given point in the trajectory is proportional to the length of the population vector. In a previous report (Schwartz 1992), an analysis of single-unit activity showed that speed information was best encoded when the direction of movement was near the cell's preferred direction. In the population algorithm, the vector contribution of a cell to the population vector is large when the movement is in the cell's preferred direction. When this condition occurs, the exact contribution will be biased by the encoded speed—the cell's contribution will be less for slower movements and greater for faster movements in the preferred direction. The cluster of cell vectors will be more round for slow portions of the movement because contributions represented by vectors oriented in the direction of movement will be shorter and more like the vectors oriented in other directions. In contrast, more elongated, asymmetrical clusters will be associated with faster portions of the movement and will result in longer population vectors. The encoding of speed is an emergent property of the population vector algorithm.

These findings also suggest that the trajectory-related information found in the motor cortex is in a specific reference frame. The tangential velocity vectors are very similar to the population vectors calculated within the drawing movement. Thus the coordinate frame depends on the trajectory tangent, moving in time and space with the finger during the task. If the reference frame had a constant origin, for instance at the shoulder, the series of population vectors would be quite different: the vectors would all fan out from the same origin and their directions would not change periodically. Because the instantaneous location in the trajectory is a necessary initial condition and the population vector precedes the actual movement, an ongoing cumulative history of the previous calculations seems to be carried out. This conclusion is based on the idea that direction is a relative parameter measured from a reference point. The data show that the direction of the population vectors when measured relative to the moving finger match the tangential velocity vectors. This was also tested for straight arm movements made through three-dimensional space in a center→out task where the same cells were recorded as the animal performed the task with three different arm orientations (Caminiti et al. 1990). The task was carried out in three different workspaces contiguous in the horizontal dimension and required a shoulder rotation of ~20° about the vertical axis for adjacent spaces. Population vectors calculated in each workspace predicted the hand direction equally well. The preferred directions of individual cells were found to be biased by shoulder orientation; the population of motor cortical neurons as a whole had a slight tendency ($r < 0.5$) to change preferred directions in the horizontal direction by ~12° for movements in adjacent work-

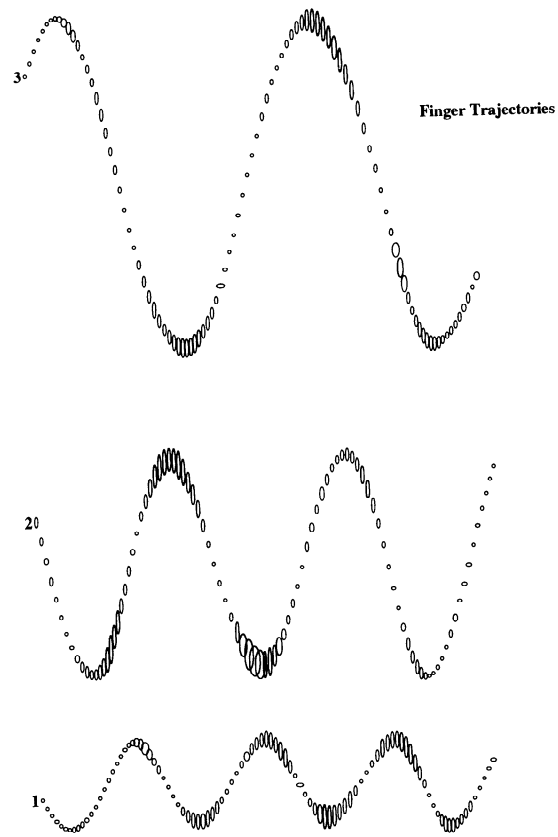

FIG. 8. Trajectory variability—classes 1–3. A bootstrap technique, described in the text, was used to calculate the variability for each bin of the finger trajectory. The x and y axes of the ellipses represent the 95% confidence interval at x and y at each position. Variability was largest at the peaks of the sinusoid. Each ellipse was scaled by a factor of 20 compared with the trajectory.

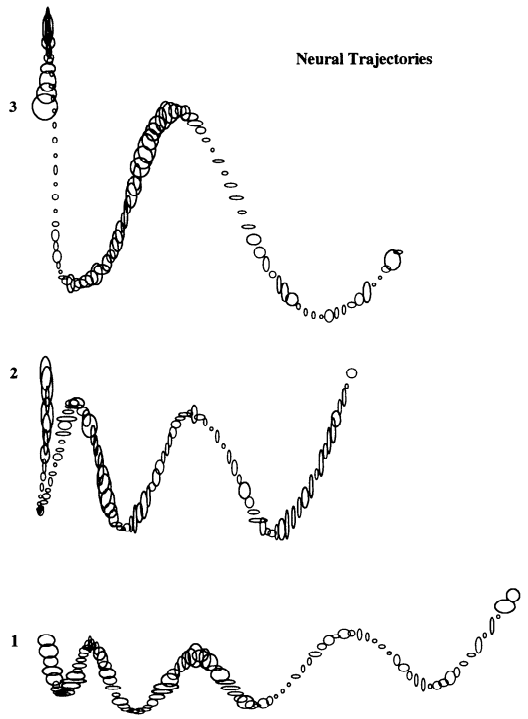

FIG. 9. Neural trajectory variability—classes 1–3. The bootstrap technique was applied to the population vectors. There was a tendency for the variability to be greater at the start of each trace. Adjacent points within a region of the trace have similar variability. The ellipses were magnified by a factor of 5 relative to the trajectory.

spaces. Although the preferred directions of individual cells may be related to shoulder posture, this was not manifest in the population vectors. The population vectors were always oriented in the same direction as the hand movement relative to the initial location of the hand.

The evolution of a volitional reaching task may be described as a sequence of coordinate transformations from a visual space to a joint-centered coordinate system (Pellionisz and Llinas 1979). For instance, Flanders et al. (1992) have suggested that, in a pointing task, the position of the target is first represented in a retinotopic coordinate system. An analysis of end-point errors for movements carried out in the dark shows that the psychophysical coordinate system is centered at the shoulder. Within a movement, target information from the retina is transformed sequentially to a head-centered, then to a shoulder-centered coordinate frame. Once transformed to the shoulder frame, the target information would then be in the same coordinate system as kinesthetically derived arm position information. Both types of information would then be joint centered and could be used to displace the arm.

This sequential process may be different for drawing movements, for which there are no discrete targets. The traced figure is probably produced by a process that relies on continuous visual guidance. The distance between the finger and the next desired location along the figure would then be the relevant input information. According to Flanders et al., this condition could "short-circuit" the series of coordinate transformations described above. The present results suggesting that information in the motor cortex is organized in a finger-centered coordinate system would support this idea. Alternatively, this information may be the result of a series of transformations that occurred before this representation was formed.

A characteristic distortion in the neural trajectories occurred at the beginning of each task, evident particularly in the six classes of sinusoid possessing the highest curvature. Most of the distortion was localized to the first peak of the figure. In this region, the population vectors were very short because the finger was moving slowly. As shown in Fig. 5, the difference between the direction of the population vector and that of the tangential velocity vector was largest in this region. Short vector magnitudes might be expected to yield less accurate directions. For example, the length of the fifteenth population vector in the class 2 sinusoid is 0.147 spikes/s. This is a very small value for the rate of discharge (derived from the population), and is smaller than the 95% confidence interval calculated from the bootstrap for that bin. (0.22 spikes/s, Fig. 9). The difference between the direction of the population and tangential velocity vector is greatest at this point (Fig. 5); the directions of the vectors before and after this matched better. Thus it is likely that the population algorithm may have limited accuracy for regions of the trajectory with high curvature (combination of slow speed and rapid change in direction). This could be a substrate for the isogony principle (Lacquaniti et al. 1983) describing the inverse relation between drawing speed and curvature. Perhaps the less distinct directional "answer" provided by the neuronal population and represented by the short population vector is indicative of a limitation of the system that controls accurate arm movement. This concept is supported by the increased variability in the more curved portions of the trajectory (Fig. 8). In general, however, the continuous prediction of direction via the population vector was accurate ($r > 0.9$, Fig. 5), even for regions of high curvature that occur later in the task. Most of the small differences between the predicted and actual direction occur within the first 15% of the task. The movement actually begins ~120 ms after the first calculated population vector, which is ~7–8% of the length of the task. The most prominent distortions occur as the displacement of the limb begins. This may be a point in the task where the sequential transformation in coordinate systems is being short-circuited as the hand starts to move and comparisons between finger location and the desired drawn figure are initiated.

The psychophysical studies of Flanders et al. also suggest that direction and distance may be processed through separate information channels. This distinction has also been found in psychophysical studies that examined the force produced in targeted isometric tasks (Favilla et al. 1989). When considered binwise, speed is the same as instantaneous distance and is coded simultaneously with direction in the same motor cortical neurons. These parameters, however, are represented differently in the discharge pattern. Direction information is broadly encoded throughout its entire range. In contrast, speed encoding occurs only for those directions of movement near the cell's preferred direction. The distinction between direction and speed is represented in the population vector as direction and magnitude. This may be an example of separate information channels contained in the same physical entity.

I thank A. Kakavand for technical assistance and Dr. J. Adams for programming support.

This work was funded by National Institute of Neurological Disorders and Stroke Grant NS-26375.

Address for reprint requests: Division of Neurobiology, Barrow Neurological Institute, 350 W. Thomas Rd., Phoenix, AZ 85013.

Received 22 September 1992; accepted in final form 17 February 1993.

REFERENCES

CAMINITI, R., JOHNSON, P. B., AND URBANO, A. Making arm movements within different parts of space: dynamic aspects in the primate motor cortex. *J. Neurosci.* 10: 2039–2058, 1990.

DIACONIS, P. AND EFRON, B. Computer-intensive methods in statistics. *Sci. Amer.* 248: 116–130, 1983.

FAVILLA, M., HENING, W., AND GHEZ, C. Trajectory control in targeted force impulses. VI. Independent specification of response amplitude and direction. *Exp. Brain Res.* 75: 280–294, 1989.

FLANDERS, M., HELMS TILLERY, S. I., AND SOECHTING, J. F. Early stages in a sensorimotor transformation. *Behav. Brain Sci.* 15: 309–362, 1992.

GEORGOPOULOS, A. P., CAMINITI, R., KALASKA, J. F., AND MASSEY, J. T. Spatial coding of movement: a hypothesis concerning the coding of movement direction by motor cortical populations. *Exp. Brain Res. Suppl.* 7: 327–336, 1983.

GEORGOPOULOS, A. P., KALASKA, J. F., CAMINITI, R., AND MASSEY, J. T. On the relations between the direction of two-dimensional arm movements and cell discharge in primate motor cortex. *J. Neurosci.* 2: 1527–1537, 1982.

GEORGOPOULOS, A. P., KETTNER, R. E., AND SCHWARTZ, A. B. Primate motor cortex and free arm movements to visual targets in three-dimensional space. II. Coding of the direction of movement by a neuronal population. *J. Neurosci.* 8: 2928–2937, 1988.

LACQUANITI, F., TERZUOLO, C., AND VIVIANI, P. The law relating kinematic and figural aspects of drawing movements. *Acta. Psychol.* 54: 115–130, 1983.

PELLIONISZ, A. AND LLINAS, R. Brain modeling by tensor network theory and computer simulation. The cerebellum: distributed processor for predictive coordination. *Neuroscience.* 4: 323–348, 1979.

SCHWARTZ, A. B. Motor cortical activity during drawing movements. Single-unit activity during sinusoid tracing. *J. Neurophysiol.* 68: 528–541, 1992.

SCHWARTZ, A. B., KETTNER, R. E., AND GEORGOPOULOS, A. P. Primate motor cortex and free arm movements to visual targets in three-dimensional space. I. Relations between single cell discharge and direction of movement. *J. Neurosci.* 8: 2913–2927, 1988.